A Novel KCNJ5-insT149 Somatic Mutation Close to, but Outside, the Selectivity Filter Causes Resistant Hypertension by Loss of Selectivity for Potassium

Maniselvan Kuppusamy, Brasilina Caroccia, Julia Stindl, Sascha Bandulik, Livia Lenzini, Francesca Gioco, Veniamin Fishman, Giuseppe Zanotti, Celso Gomez-Sanchez, Michael Bader, Richard Warth, and Gian Paolo Rossi

Department of Medicine-DIMED (M.K., B.C., L.L., F.G., G.P.R.), Department of Internal Medicine 4, and Department of Biomedical Sciences (G.Z.), University of Padua, 35126 Padua, Italy; Department of Medical Cell Biology (J.S., S.B., R.W.), University of Regensburg, 93053 Regensburg, Germany; Max Delbrück Center for Molecular Medicine (V.F., M.B.), 13092 Berlin, Germany; Division of Endocrinology (C.G.-S.), G. V. (Sonny) Montgomery Veterans Affairs Medical Center and Department of Medicine, University of Mississippi Medical Center, Jackson, Mississippi 39216

Context: Understanding the function of the KCNJ5 potassium channel through characterization of naturally occurring novel mutations is key for dissecting the mechanism(s) of autonomous aldosterone secretion in primary aldosteronism.

Objective: We sought for such novel KCNJ5 channel mutations in a large database of patients with aldosterone-producing adenomas (APAs).

Methods: We discovered a novel somatic c.446insAAC insertion, resulting in the mutant protein KCNJ5-insT149, in a patient with severe drug-resistant hypertension among 195 consecutive patients with a conclusive diagnosis of APA, 24.6% of whom showed somatic KCNJ5 mutations. By site-directed mutagenesis, we created the mutated cDNA that was transfected, along with KCNJ3 cDNA, in mammalian cells. We also localized CYP11B2 in the excised adrenal gland with immunohistochemistry and immunofluorescence using an antibody specific to human CYP11B2. Whole-cell patch clamp recordings, CYP11B2 mRNA, aldosterone measurement, and molecular modeling were performed to characterize the novel KCNJ5-insT149 mutation.

Results: Compared with wild-type and mock-transfected adrenocortical cells, HAC15 cells expressing the mutant KCNJ5 showed increased CYP11B2 expression and aldosterone secretion. Mammalian cells expressing the mutated KCNJ5-insT149 channel exhibited a strong Na^+ inward current and, in parallel, a substantial rise in intracellular Ca^{2+}, caused by activation of voltage-gated Ca^{2+} channels and reduced Ca^{2+} elimination by Na^+/Ca^{2+} exchangers, as well as an increased production of aldosterone.

Conclusions: This novel mutation shows pathological Na^+ permeability, membrane depolarization, raised cytosolic Ca^{2+}, and increased aldosterone synthesis. Hence, a novel KCNJ5 channelopathy located after the pore α-helix preceding the selectivity filter causes constitutive secretion of aldosterone with ensuing resistant hypertension in a patient with a small APA. **(*J Clin Endocrinol Metab* 99: E1765–E1773, 2014)**

Primary aldosteronism (PA) detrimentally affects the cardiovascular system (1). It is a common cause of high blood pressure (BP), particularly in patients who are resistant to drug treatment (2). From one third to two thirds of the PA cases, depending on whether the adrenal vein sampling is systematically used, can be attributed to

ISSN Print 0021-972X ISSN Online 1945-7197
Printed in U.S.A.

Received April 2, 2014. Accepted May 29, 2014.
First Published Online June 24, 2014

Abbreviations: APA, aldosterone-producing adenoma; BP, blood pressure; HEK293, human embryonic kidney-293; LV, left ventricular; PA, primary aldosteronism.

an aldosterone-producing adenoma (APA) (2). The hallmark of this is an autonomous overproduction of aldosterone: angiotensin II, one of the best known secretagogues of aldosterone, is in fact low to undetectable in PA plasma (3).

This functional autonomy remained mechanistically unexplained until somatic mutations of the G protein-activated inwardly rectifying K^+ channel Kir3.4, one of four identified Kir3 channels and encoded by the *KCNJ5* gene, were discovered (4). These mutations are located in, or close to, the selectivity filter (4, 5), a highly conserved region within this family of channels that allows the selective transport of K^+ over other cations (4). The channel protein forms homo- or heterotetrameric complexes, mainly with Kir 3.1 (KCNJ3) and less commonly also with Kir3.2 (KCNJ6) or Kir3.3 (KCNJ9). An extracellular pore-forming region links these complexes that have intracellular N- and C-terminal domains and two membrane-spanning domains (6).

A considerable proportion APAs, varying from 30% to 60%, depending on gender and ethnicity, carries a mutation of the selectivity filter of the KCNJ5 channels (7–10). Along with the TWIK (Tandem of P domains in a Weak Inward rectifying K+ channel)-related acid sensitive K^+ channels (11, 12), these channels are expressed in the human adrenocortical zona glomerulosa cells and contribute to maintaining these cells hyperpolarized (4). Hyperpolarization blunts the open probability of T-type Ca^{2+} channels (13) and by this mechanism maintains low intracellular Ca^{2+} levels, low Ca^{2+}-calmodulin pathway activation, and low expression levels of CYP11B2, the last enzyme for aldosterone production (5).

Given the multiple effects of intracellular Ca^{2+} on adrenocortical steroidogenesis, these channels are now held to play a key role in regulating aldosterone secretion (13). Accordingly many aldosterone secretagogues, such as angiotensin II and endothelin-1 (14, 15), decrease the expression of the KCNJ5 channel mRNA and protein, causing blunted channel activity. The resulting membrane depolarization increases intracellular Ca^{2+} and stimulates aldosterone production. In APA, somatic mutations of the KCNJ5 selectivity filter also induce increased CYP11B2 expression, constitutive aldosterone secretion (11), and an excess left ventricular (LV) hypertrophy (16).

We herein report on identification of a novel somatic KCNJ5 mutation consisting of insertion of a threonine residue close to, but just outside of, the Kir3.4 selectivity filter in an APA patient presenting with drug-resistant hypertension. Because the electrophysiological consequences of such novel naturally occurring mutations can contribute to the understanding of how this channel function, we also report on the effects of this mutation on membrane potential, intracellular calcium and the current-voltage relationship in whole-cell studies.

Materials and Methods

APA genotyping

DNA was extracted from APAs removed from 195 consecutive APA patients from two Italian referral centers (Padua and Rome) that perform similar systematic screening of newly diagnosed hypertensive patients and sequenced as described (please see Supplemental Material) to identify KCNJ5 mutations.

Clinical case

The patient was a 65-year-old man referred for long-standing (11 y) drug-resistant hypertension, which had already caused a stroke in 2000. On presentation his BP was 183/102 mm Hg supine and 170/101 mm Hg standing despite full adherence to treatment with canrenone 50 mg/d, telmisartan 80 mg/d, nebivolol 10 mg/d, doxazosin 2 mg/d, and amlodipine 10 mg/d. His serum K^+ was 2.5 mEq/L; renin was suppressed [direct renin 3.0 μU/mL supine; 2.3 μU/mL standing (17), and his plasma aldosterone concentration was 37.4 ng/dL supine and 61.5 ng/dL standing (n.v. <15 ng/dL and <25 ng/dL, respectively] (18). He did not tolerate higher canrenone doses because of erectile dysfunction.

After he had an echocardiogram, he was found to have concentric LV hypertrophy [LV mass index 171 g/m^2 (normal values <115 g/m^2); relative wall thickness 0.56 (n.v. <0.45]. On a computed tomography, a 9-mm (maximum diameter) nodule was seen in his right adrenal gland. Hormonal retesting after adequate washout from interfering drugs (3), while he was only on doxazosin 4 mg/d and slow-release verapamil 180 mg/d, showed a plasma renin activity of 0.20 ng/mL·h, both baseline and postcaptopril, and plasma aldosterone concentration of 36.4 ng/dl basally and 31.3 ng/dL postcaptopril. Hence, the aldosterone/renin ratio (ARR) was markedly elevated [182 baseline; 156 after captopril (n.v. <26 and <13.7, respectively, as determined in the Primary Aldosteronism Prevalence in hYpertension (PAPY) study (2)]. He therefore underwent adrenal vein sampling that was bilaterally selective (selectivity index >3) and showed a right lateralization index of 3.49, indicating right lateralization. After a laparoscopic right adrenalectomy, a small adenoma was found. After 2 years of follow-up, there was an impressive regression of LV hypertrophy and only concentric remodeling was still evident (LV mass index 109 g/m^2; relative wall thickness 0.47). The ARR is 5 and the serum K^+ is 4.3 mEq/L, and at 24 hours of ambulatory BP monitoring, his BP is 132/70 mm Hg while on amlodipine 5 mg/d and nebivolol 5 mg b.i.d. Thus, concomitance of the long-term cure of the hyperaldosteronism, the regression of target organ damage, and the prominent decrease of his BP that became responsive to treatment, alongside AVS and pathology data, in retrospective allowed a conclusive diagnosis of APA by the four corners criteria (2).

Immunohistochemistry

We performed immunohistochemistry using CYP11B2 and CYP11B1 antibodies (19). Paraffin-embedded adrenal was cut at 5 μm and the sections dried and then melted at 56°C for at least

3 hours. After deparaffination through alcohols, slides were subjected to antigen retrieval using Trilogy (Cell Marque Corp) in autoclave, 15 minutes at 121°C, and then treated with phenylhydrazine 0.1% for 20 minutes to inhibit endogenous peroxidases. Slides were blocked with Tris 0.1 M, goat serum 5%, or horse serum 5%, SDS 0.5% (pH 7.4) for 1 hour, and then incubated with CYP11B2 antibody (hCYP11B2-41-17B clone 1:500 dilution) or both CYP11B1 (CYP11B1-80-7-5 clone 1:200 dilution) and CYP11B2 (hCYP11B2-41-17B clone 1:500 dilution) overnight at 4°C. After washing, slides were incubated with secondary antibodies for 1 hour at room temperature. We used mouse Polink-2 Plus HRP (GBI Labs) for CYP11B2 immunostaining; rat Polink-2 Plus AP (GBI Labs), and ImmPRESS antimouse Ig reagent (Vector Laboratories) for double immunostaining. Slides were developed using diaminobenzidine and HighDef green immunohistochemistry chromogen AP (Enzo Life Sciences). All the samples were counterstained with Meyer hematoxylin (Vector Laboratories) before mounting.

Immunofluorescence

Triple immunofluorescence was done using CYP11B1, CYP11B2, and 17α-hydroxylase (20) antibodies. The protocol we followed was the same as that for the double immunohistochemistry. The detailed method is described in the Supplemental Methods.

Plasmids

For studies of CYP11B1 and CYP11B2 expression and aldosterone production, adrenocortical HAC15 were transfected with human full-length cDNA of KCNJ3 (SC118769; Origene) and of KCNJ5 (SC119590), in which the KCNJ5 mutations (T158A and insT149) were inserted using the QuikChange II XL site directed mutagenesis kit (Stratagene).

For electrophysiology studies and Ca^{2+} measurements, the following plasmid constructs were used: human wild-type KCNJ3 and KCNJ5 cDNAs were purchased from Invitrogen/Geneart, Life Technologies GmbH. The mutation c.446insAAC of KCNJ5 (resulting in the mutant protein KCNJ5-insT149) was generated by site-directed mutagenesis in the human KCNJ5 cDNA. KCNJ5 cDNAs and KCNJ3 cDNAs were subcloned into the bicistronic expression vector pIRES-CD8 (21). Details of both plasmid constructs are given in the Supplemental Methods.

RNA extraction and quantitative RT-PCR

Total RNA was extracted with the RNAeasy kit (QIAGEN); its integrity and quality were verified with a lab-on-chip technology in an Agilent Bioanalyzer 2100 with the RNA6000 Nano assay (Agilent Technologies). Quantitative RT-PCR using the universal Probe Library and specific primers as described (22). The detailed method (Supplemental Table 1) is provided in the Supplemental Methods.

Electrophysiological characterization of the KCNJ5-insT149 mutant

Patch-clamp recordings were performed using an EPC-10 amplifier without leak subtraction (HEKA) as described in the Supplemental Methods.

Ca^{2+} measurements

Cytoplasmic Ca^{2+} was measured using adrenocortical carcinoma NCI-H295R cells transfected with wild-type KCNJ5 or mutant KCNJ5-insT149 and preloaded with the Ca^{2+}-sensitive dye Fura-2 (Molecular Probes) as described in detail in the Supplemental Methods. All the experiments were performed at room temperature.

Aldosterone measurement

Seventy-two hours after transfection, the cell culture medium was collected for aldosterone measurement (with the aldosterone ELISA kit from Alpha Diagnostic International) as described in the Supplemental Material.

Molecular modeling of the KCNJ5-insT149 mutant

A model of the KCNJ5 tetramer, amino acids from 51 to 370, was built by homology modeling with the web server Swiss-Model (23). The latter presents 85% sequence identity with KCNJ5. A threonine was inserted at position 149 with the graphic program Coot (24) and the model adjusted by hand and optimized by molecular dynamics with software CNS (25) (for detailed method, please see Supplemental Data).

Statistical analysis

Results were expressed as mean ± SEM of at least three separate experiments in which each sample was assayed in triplicate or quadruplicate. Differences between groups were analyzed by *t* test and, for multiple group comparison, by one-way ANOVA followed by Bonferroni's comparisons. The differences were considered to be significant at $P < .05$. Statistical analyses were performed using GraphPad/Prism version5 for Windows software (GraphPad Software, www.graphpad.com).

Results

Sequencing of KCNJ5

Somatic mutations of KCNJ5 were detected in 48 of the 195 consecutive patients with a conclusive diagnosis of APA who were sequenced (24.6%) (Supplemental Table 2). All but one of these mutations were already known (Table 1). A novel somatic c.446insAAC insertion resulting in the mutant protein KCNJ5-insT149 (Supplemental Figure 1) was identified in a patient with severe drug-resistant hypertension.

Immunohistochemistry and double immunofluorescence

The patient carrying the KCNJ5-insT149 mutation had a small adrenal adenoma that stained strongly and in a fairly uniform pattern with the CYP11B2 antibody (Figure 1A). There was an area of strong staining distant from the adenoma, one section of which had scattered cells and the other larger section had relatively compact staining (Figure 1, B and C). Double staining showed that the CYP11B1 (green) was localized to cells surrounding the adenoma, and there were a few cells expressing the

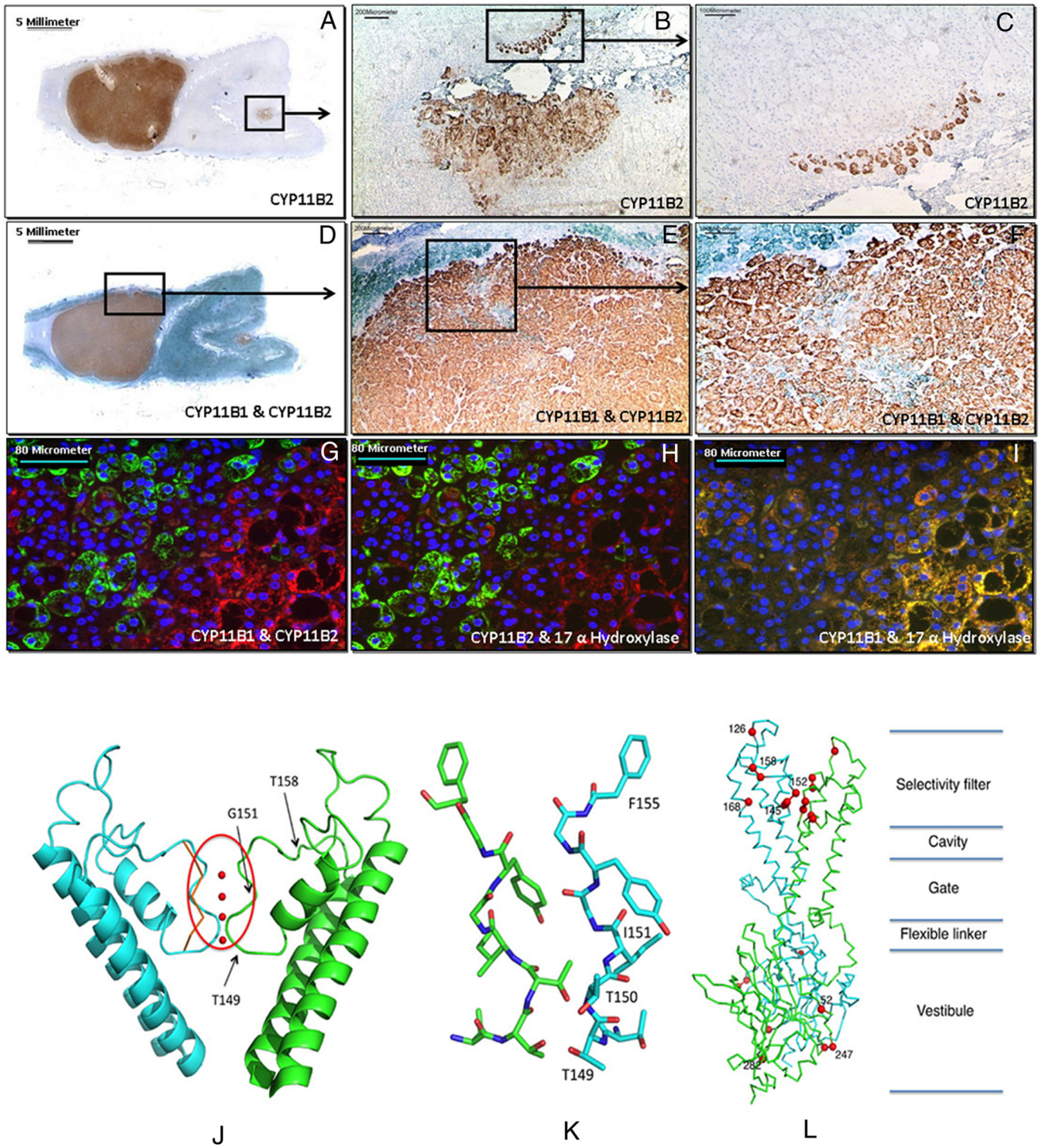

Figure 1. CYP11B1 and CYP11B2 adrenal immunohistochemistry and triple immunofluorescence for CYP11B1, CYP11B2, and 17α-hydroxylase: panels A–C are different areas at higher magnification of the same adrenal stained with the hCYP11B2-41-17B antibody. Panels D–F are double staining for CYP11B1-80-7-5 (green) and CYP11B2 (brown) antibodies. Panels G–I are images of triple immunofluorescence for CYP11B1, CYP11B2, and 17α-hydroxylase at the same magnification ($\times$10). Panels G–I are the merged image of CYP11B2 (green) and CYP11B1 (red) staining, CYP11B2 (green) and 17 α-hydroxylase (red), and CYP11B1 (green) and 17 α-hydroxylase (red), respectively. Panel J shows a cartoon drawing of the selectivity region of KCNJ5-insT149 mutant after molecular dynamics model optimization. Only two chains of the tetramer, cyan and green, are shown for clarity purposes. A red oval encloses the amino acids directly involved in the interaction with K^+ ions. The position of the Cα's of the selectivity filter residues in the original crystal structure is shown in orange. Small red spheres represent K^+ ions as present in the crystal structure of the KCNJ12 channel (PDB code 3SYA). The position of the inserted threonine along with that of two mutations previously found (4) is indicated by arrows. Panel K shows all the atoms of residues from 148 to 155 after the molecular dynamics simulation (as in the previous panel, only two chains are shown). The insertion of Thr149 perturbs the filter residues, and now the two carbonyl oxygen of Thr150 and Ile151 point far from the filter cavity, whereas the $-$OH of Thr149 protrudes in it. Panel L shows a ribbon drawing of the KCNJ5148 model with all mutations. Red spheres localize residues bearing mutations until now identified in primary aldosteronism. Only two polymeric chains are shown for clarity purposes. Classification of the different portion of the channel is reported, with respect to the green subunit (39, 40).

CYP11B1 within the adenoma (Figure 1, D–F). Triple immunofluorescence showed that the CYP11B1 and the CYP11B2 did not colocalized within the same cells, but there were CYP11B1 cells in between cells expressing the CYP11B2 enzyme (Figure 1G). The CYP11B2 did not colocalize with the 17α-hydroxylase, but the CYP11B1 colocalized with the 17α-hydroxylase (Figure 1, H and I).

Molecular modeling of the KCNJ5-insT149 mutant

The model of the KCNJ5 tetramer, amino acids from 51 to 370, built by homology modeling of this novel mutation, showed that the inserted threonine 149 residue is located after the pore α-helix that precedes the selectivity filter of the K^+ channel (Figure 1, J–L). This insertion places the threonine residue at the beginning of the filter sequence, altering its geometry (26). The K^+ path through the filter is guided by a line of three main chain carbonyl oxygen atoms facing the channel pore, plus the hydroxyl group of a threonine. The insertion of a residue at one end of the pore displaces two of these carbonyls, producing a widening of the pore space. At the same time, the −OH group of the side chain of a second threonine protrudes into the channel pore.

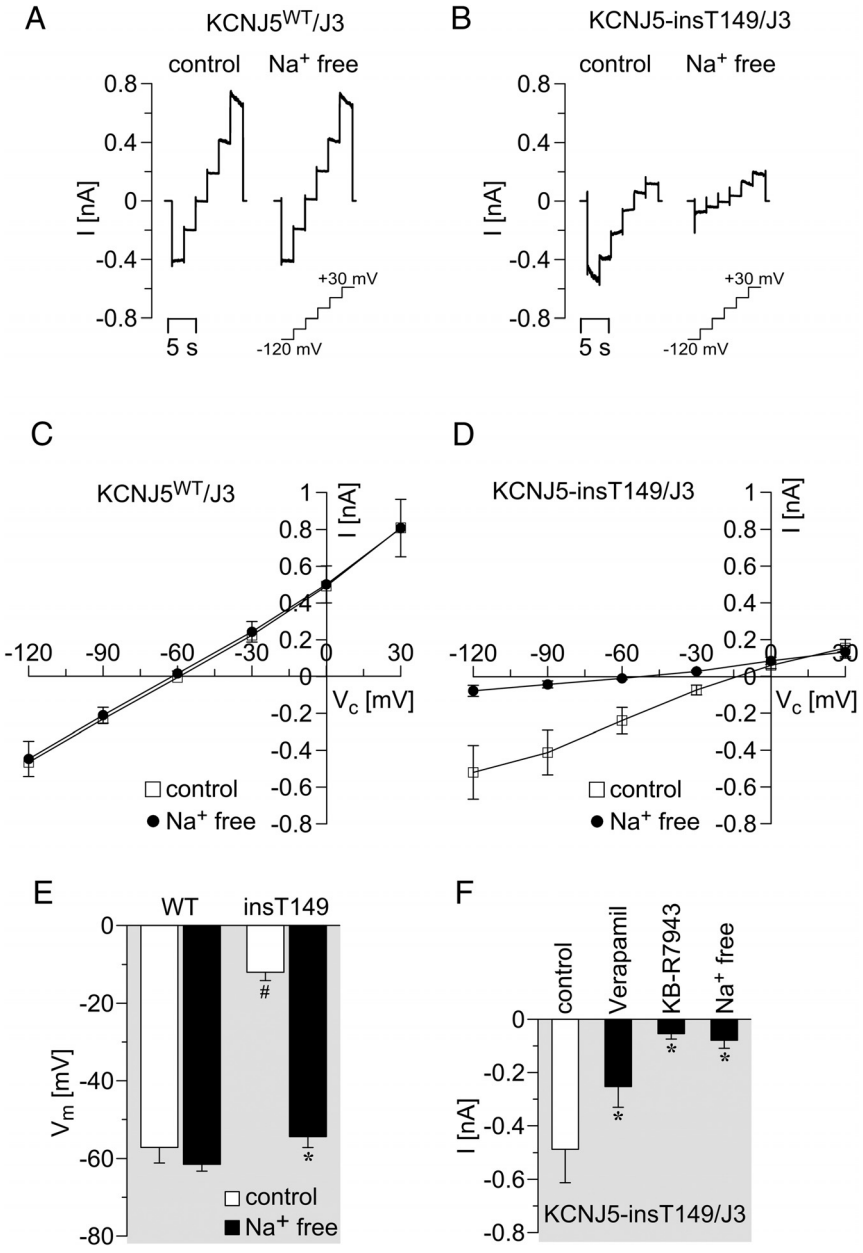

Figure 2. Electrophysiological characterization of the KCNJ5-insT149 mutant: basic characteristics of the KCNJ5-insT149 mutant channel in HEK293 cells. Typical original whole-cell current traces of a wild-type KCNJ5/KCNJ3 (KCNJ5WT/J3) (A) and a mutant KCNJ5-149insAAC/KCNJ3 (KCNJ5-insT149/J3) expressing HEK293 cells (B) are shown. Current traces were recorded in the presence of extracellular Na^+ (control) and after replacement of extracellular Na^+ by $NMDG^+$ (Na^+ free). C and D, Summary of I/V curves of similar whole-cell experiments as shown (A and B) (KCNJ5WT/J3, n = 8; KCNJ5insT149/J3, n = 7). E, Effect of Na^+ replacement on the membrane voltage. *, $P < .05$ control vs Na^+ free; #, $P < .05$ KCNJ5WT (n = 8) vs KCNJ5insT149 (n = 7). F, Inhibition of the inward current (at −120 mV) in HEK293 cells transfected with KCNJ5-insT149/J3. Verapamil (10 μM, n = 6) inhibited approximately 50% of the inward current. KB-R7943 (10 μM, n = 4) abolished the inward current, an effect similar to the removal of Na^+-free bath solution (n = 8). *, $P < .05$, experimental vs control condition; #, indicates $P < .05$ KCNJ5WT vs KCNJ5-insT149. Values are mean values ± SEM.

Mutant KCNJ5-insT149 K^+ channels are Na^+ permeable and lead to increased intracellular free calcium concentration

The electrophysiological consequences of the KCNJ5-insT149 mutation were analyzed in human embryonic kidney-293 (HEK293) cells that were transiently cotransfected with mutant or wild-type KCNJ5 together with KCNJ3, a subunit that assembles with KCNJ5 to form native channels.

In whole-cell patch-clamp experiments, wild-type KCNJ5/KCNJ3-transfected cells showed inward (negative) and strong outward (positive) currents, depending on the voltage clamped. The outward currents mainly reflected K^+ efflux through K^+ channels. Whole-cell currents of these cells were not changed by replacing bath Na^+ with the larger cation $NMDG^+$ (Na^+ free; Figure 2, A and C).

In cells expressing mutant KCNJ5T-ins149/KCNJ3 channels, the inward currents were larger, and the outward currents were blunted. Replacement of extracellular Na^+ by N-methyl-D-glucamine almost abolished the inward currents, thus indicating that they were caused by a pathological Na^+ influx through mutated KCNJ5 channels (Figure 2, B and D). The pathological Na^+ influx led to a depolarization of the membrane voltage of cells transfected with the mutant KCNJ5-insT149/KCNJ3 compared with cells transfected with the wild-type channels (Figure 2E). Removal of bath Na^+ led to a strong hyperpolarization of cells transfected with the mutant channels.

APA-associated mutations of KCNJ5 lead to a modified pharmacology (4): for instance, the KCNJ5-L168R mutant is inhibited by blockers of Na^+ transporting proteins and voltage-gated Ca^{2+} channels (27). In HEK293 cells transfected with KCNJ5-insT149/KCNJ3, the L-type Ca^{2+} channel blocker verapamil (10 μM) inhibited some 50% of the pathological Na^+ inward current; the Na^+/Ca^{2+} exchanger blocker KB-R7943 (10 μM) inhibited the Na^+ inward current completely, similar to the removal of Na^+ from the bath solution (Figure 2F and Supplemental Figure 2).

In aldosterone-producing adrenal cells, membrane depolarization causes the opening of voltage-gated Ca^{2+} channels and a rise of intracellular Ca^{2+} that is key for the stimulation of aldosterone synthesis. Therefore, we examined the effect of the adenoma-associated KCNJ5-insT149 mutant on cytosolic Ca^{2+} activity in adrenocortical carcinoma NCI-H295R cells. Cytosolic Ca^{2+} activity, as measured by the Fura-2 ratio (340/380 nm), was increased in KCNJ5-insT149 expressing cells compared with cells with wild type KCNJ5 (Figure 3A). Compared with nontransfected cells of the same dishes (Figure 3A, n.t.), resting cytosolic Ca^{2+} was slightly decreased in cells expressing wild-type KCNJ5, suggesting that wild-type KCNJ5 hyperpolarizes the membrane and reduces Ca^{2+} influx across the plasma membrane. Removal of bath Na^+ caused a strong rise in intracellular Ca^{2+} in NCI-H295R cells expressing the KCNJ5-insT149 mutant but not in wild-type KCNJ5-transfected cells. Verapamil (10 μM) reduced intracellular Ca^{2+} only slightly (Figure 3B).

Aldosterone measurement

Seventy-two hours after transfection with expression constructs for wild-type and mutated KCNJ5 (insT149 and T158A) together with KCNJ3, HAC15 cells showed no change of CYP11B1 expression, whereas both KCNJ5 mutants exhibited increased CYP11B2 expression ($P < .001$) and aldosterone production ($P < .01$) as compared with both mock-transfected and KCNJ5 wild-type transfected HAC15 cells (Figure 4 , A–C, and Supplemental Table 3).

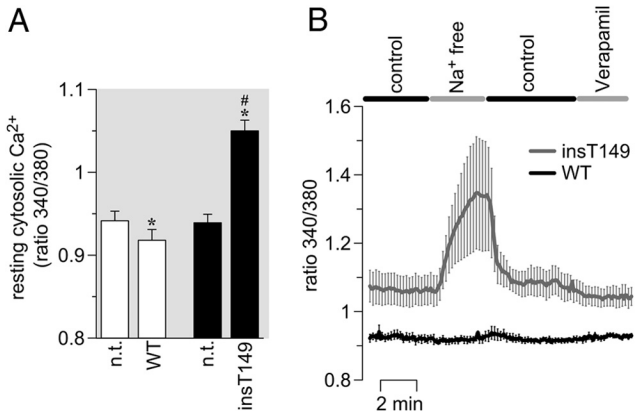

Figure 3. Influence of the mutated KCNJ5 on the Ca^{2+} homeostasis in adrenocortical carcinoma NCI-H295R cells. A, Ca^{2+} activity of NCI-H295R cells, as measured by Fura-2 ratios, were higher in KCNJ5insT149 cells (nine transfected cells and 13 nontransfected (n.t.) cells from four independent dishes), compared with wild-type KCNJ5 expressing cells [seven transfected cells and 10 nontransfected (n.t.) cells from four independent dishes]. *, $P < .05$ nontransfected vs KCNJ5-WT or KCNJ5-insT149 transfected cells; #, $P < .05$ KCNJ5-WT vs KCNJ5-insT149. Values are mean ± SEM. B, Effect of Na^+-free bath solution and verapamil (10 μM) on Fura-2 ratios of KCNJ5-insT149 (n = 6 cells from three independent dishes) or KCNJ5-WT (n = 6 cells from three independent dishes)-transfected NCI-H295R cells.

Discussion

The electrophysiological characterization of novel naturally occurring mutations of the KCNJ5 channel at sites in the channel different from the selectivity filter can be key for a better understanding of the function of this channel. Most KCNJ5 mutations reported thus far in APA patients (4, 8–10, 28–37) (Table 1) entailed a substitution of amino acid residues in the selectivity filter (Figure 1L) (5), and caused enhanced aldosterone secretion (11), due to an increased expression of CYP11B2 in the tumor and enhanced aldosterone secretion in the adrenal vein blood draining from it (22).

We have herein identified a novel KCNJ5 somatic mutation in a patient presenting with drug-resistant hypertension due to an APA that was unequivocally proven to express the *CYP11B2* gene using a monoclonal antibody developed for the human aldosterone synthase (Figure 1, A–I). This unique mutation consists of insertion of one threonine 149 residue at the end of the pore α-helix that precedes the selectivity filter of the K^+ channel (Figure 1, J–L). We show that addition of this threonine residue significantly alters the geometry of the filter and, like the mutations in the filter or in close proximity (Table 1), modifies the channel selectivity, destroys its selectivity for the K^+, and eventually produce nonselective channels (26).

Studies in the human adrenocortical HAC15 cells transfected with the mutant KCNJ5-insT149 together with KCNJ3, a subunit that assembles with KCNJ5 to form native channels, support this hypothesis. They showed increased expression of the *CYP11B2* (but not the *CYP11B1*) gene,

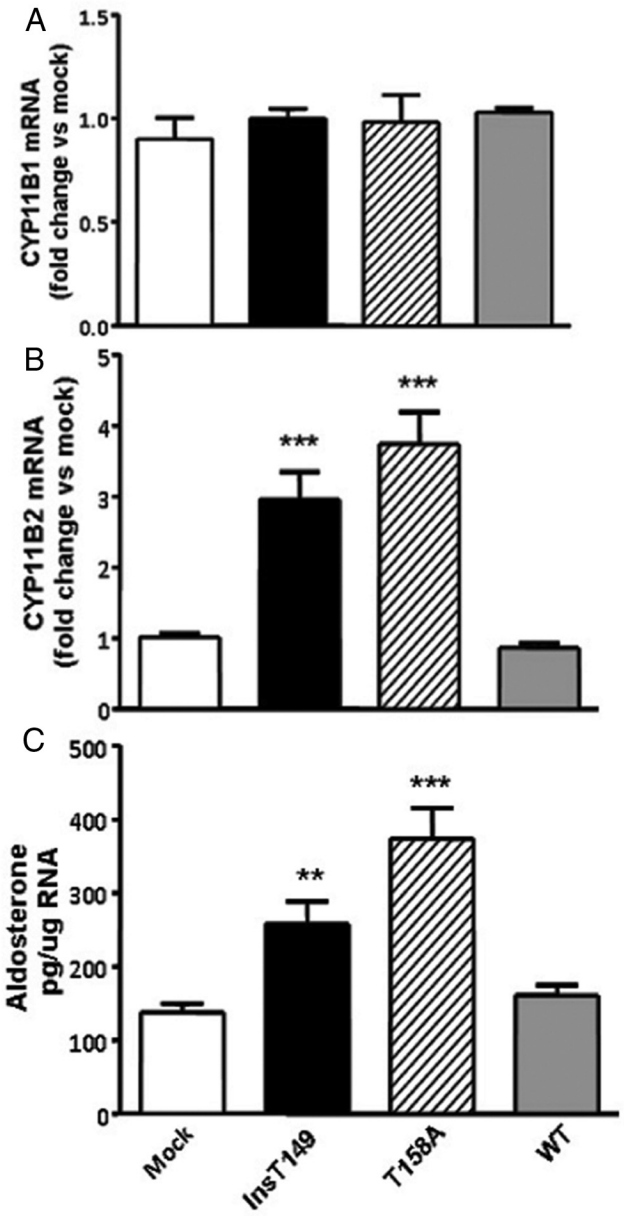

Figure 4. Effect of KCNJ5-insT149 mutation on CYP11B2 and CYP11B1 expression and aldosterone production: HAC15 cells transiently transfected with either the control (mock transfected) or one of the mutant KCNJ5. A, CYP11B1 mRNA expression. B, CYP11B2 mRNA expression. C, Aldosterone release. Results were shown as mean ± SEM (n = 6). ***, $P < .001$ and **, $P < .01$ vs mock and wild type.

and augmented aldosterone production compared with mock-transfected cells and to cells transfected with the wild-type channel (Figure 4, A–C).

We further characterized the functional consequences of this novel mutation in whole-cell patch-clamp experiments in HEK293 cells. Cells cotransfected with KCNJ5-insT149/KCNJ3 were depolarized; moreover, they exhibited a strong Na^+ inward current consistent with a pathological loss of K^+ selectivity of the mutant channel. The novel mutant KCNJ5-insT149, similar to the mutant KCNJ5-L168R (27), was inhibited by KB-R7943, an inhibitor of Na^+/Ca^{2+} exchangers, and also by the Ca^{2+} channel blocker verapamil. However, with an IC_{50} of about 10 μM, the mutant KCNJ5-insT149 was less verapamil sensitive compared with KCNJ5-L168R (IC_{50} of about 1.2 μM). Verapamil at clinically used doses (38) yields plasma concentrations in the low micromolar range and therefore, probably, does not affect KCNJ5-insT149 in a relevant way in vivo. However, it might reduce the Ca^{2+} influx through Ca^{2+} channels activated by the mutant KCNJ5-induced depolarization. Hence, further clinical studies on APA patients are needed to investigate the effect of verapamil in diagnostic and therapeutic settings in patients harboring KCNJ5 mutations.

We found that the novel KCNJ5-insT149 mutation, like other APA-associated KCNJ5 mutations, led to a pathological increase in cytosolic Ca^{2+}. This rise in Ca^{2+} appears to be induced by several mechanisms: 1) depolarization of the membrane leads to activation of voltage-gated Ca^{2+} channels; and 2) some permeability of the mutant channel itself for Ca^{2+} [as observed for KCNJ5-G151E (29)]. The cell depolarization and rise in intracellular Na^+ also reduce the driving force of Ca^{2+} elimination via Na^+/Ca^{2+} exchangers and, if strong enough, might induce a reversed mode of such exchangers. At present, it is not clear whether Na^+ loading and depolarization of native adenoma cells with mutated KCNJ5 are strong enough to permit the reversed mode of Na^+/Ca^{2+} exchangers. If so, in the future more specific inhibitors of Na^+/Ca^{2+} exchangers could be a strategy to lower intracellular Ca^{2+} of adenoma cells.

Taken together, these results indicate that similar to other APA-associated KCNJ5 mutations, the KCNJ5-insT149 mutation conferred a pathological Na^+ permeability to the channel resulting in cell depolarization, and activation of Ca^{2+} influx. The latter probably promotes stimulation of aldosterone synthesis and possibly adenoma formation. Fourteen other mutated (or deleted) positions were previously found in PA patients (10 in selectivity filter of KCNJ5 and four away from it; Figure 1L). Of them, only two (151 and 152) involve residues directly overlooking the selectivity filter: wild-type residue 151 is a glycine and both mutations (G151R and G151E) introduce a cumbersome charged side chain in an already crowded area, thus strongly perturbing the filter from the standpoint of both size and charge. Accordingly, both mutations were functionally described to alter ion conductivity and depolarize the membrane (Table 1). Mutation Y152C has an opposite conformational effect because a bulky side chain that points in the opposite direction with respect to the ion channel is substituted by a smaller one (31). The −OH group of tyrosine 152 forms an H-bond interaction with threonine 146 (4); the loss of the interaction, coupled to the vacuum generated by the substitution desta-

Table 1. The Kir3.4 (KCNJ5) K^+ Channel Mutations Identified Thus Far Listed According to Their Location

				Demonstrated Effects						
Amino Acid Change	Nucleotide Change	rs Number	Mutation Status G/S[a]	Increased Na^+ Conductance	Loss of K^+ Selectivity	Increased Ca^{2+} Influx	Membrane Depolarization	Increased CYP11B2 mRNA	Increased Aldosterone Production	Reference Number
R52H[a]	G155A	rs144062083	S	Y	Y	NA	NA	NA	Y	37
W126R	T376C	–	S	NA	NA	NA	NA	Y	NA	30
E145Q	G433C	–	S	NA	NA	NA	NA	NA	NA	8
E145K	G433A		S	NA	NA	NA	NA	NA	NA	34
InsT149	**446insAAC**	–	**S**	**Y**	**Y**	**Y**	**Y**	**Y**	**Y**	
G151R	G451A or C	rs386352319	G or S	Y	Y	Y	Y	Y	NA	4, 27, 29, 32, 33
G151E	G452A	–	G	Y	Y	Y	Y	NA	NA	28, 29
Y152C	A455G	–	G	Y	Y	Y	Y	Y	NA	31
I157S	T470G	–	G	Y	Y	NA	Y	NA	NA	36
del T157	467_469delTCA	rs200717351	S	Y	Y	NA	Y	NA	Y	33, 35, 37
T158A	A472G	rs387906778	G	Y	Y	Y	Y	Y	Y	4, 11
L168R	T503G	rs386352318	S	Y	Y	Y	Y	Y	NA	4, 27, 32, 33
E246K[a]	G736A	–	S	Y	Y	NA	Y	NA	Y	37
G247R[a]	G739A	rs200170681	S	–	–	NA	–	NA	–	37
E282Q[a]	C844G	rs7102584	S	Y	Y	NA	Y	NA	Y	37

Abbreviations: G, germline mutation; NA, not available; –, no; S, sporadic mutation; Y, yes. The mutation identified in this study is shown in bold.

[a] Mutations are located far from the KCNJ5 selectivity filter.

bilizes the selectivity filter, as demonstrated by the functional effects on ion conductance.

Another five mutated positions (126, 145, 157, 158, and 168) localize in the selectivity filter domain but not directly in contact with the ion tunnel. The L168R had the most marked effect: the introduction of a positively charged side chain in a mostly hydrophobic environment strongly perturbs the three-dimensional structure and thus the channel conductance. The conformational effects of the T158A substitution are less evident, but the presence of an H-bond between the −OH group of threonine and the carbonyl oxygen of proline 128 in the native structure suggests some destabilization of the structure and of the overall domain. The relevance of this portion of the selectivity filter region is also supported by the deletion of position 157 or its mutation from isoleucine to serine (33, 35, 36), which also affects conductivity (Table 1). Substitution E145Q, despite being conservative with respect to the size of the side chain, destroys the potential salt bridge between glutamic acid 145 and arginine 155 (8, 34). Finally, the only known consequence of the replacement of tryptophan 126, which is located on a loop of the selectively filter region fully exposed to the solvent, with an arginine is a modification of the electrostatic potential of the local surface (30). The remaining four mutated positions (52, 246, 247, and 282) are in the vestibule domain of the KCNJ5 channel (37) (Figure 1L), which has been proposed to be a key component of the gating mechanism (39).

The mutations (Table 1) have been found to increase Na^+ conductance and to loose K^+ selectivity. Mutations E246K, G247R, and E282Q involve residues located on the surface of the vestibule domain, and they can be easily accommodated with minor local rearrangements, the only known consequence being a modification of the local electrostatic potential. The effects of mutation R52H are more complex because arginine 52 located at the N terminus of the protein forms a salt bridge with glutamic acid 326 and H bonds with carbonyl oxygen of serine 321 and methionine 54. In this way it helps to bind the N terminus of the protein to the C-terminal vestibule domain. Substitution of this residue with a histidine weakens this interaction, with unpredictable conformational effects on the K^+ transport process.

In conclusion, we provided the following novel pieces of evidence: a threonine insertion at the end of the pore α-helix before the selectivity filter of the K^+ channel causes loss of K^+ selectivity, Na^+ permeability, and Ca^{2+} influx via opening of voltage-activated T-type and L-type calcium channels (4, 5, 11) and impairment of Na^+/Ca^{2+} exchangers, leading to enhanced CYP11B2 expression and a constitutive oversecretion of aldosterone from the tumor. The prevalence of this novel mutation, which has unequivocal functional consequences, needs to be investigated further, particularly in patients presenting, as this case, with drug-resistant hypertension with the aim to determine whether this novel mutation occurs also as a germline mutation.

Acknowledgments

We thank the Foundation for Advanced Research in Hypertension and Cardiovascular Diseases (www.forica.it). No relationship with industry is to be disclosed.

Address all correspondence and requests for reprints to: Professor Gian Paolo Rossi, MD, FACC, FAHA, DMCS, Department of Internal Medicine 4, University Hospital, Via Giustiniani, 2, 35126 Padova, Italy. E-mail: gianpaolo.rossi@unipd.it.

This work was supported by The Foundation for Advanced Research in Hypertension and Cardiovascular Diseases (www.forica.it),

the Società Italiana dell'Ipertensione Arteriosa, and the University of Padua (to G.P.R.); Deutsche Forschungsgemeinschaft Grant FOR 1086 (to S.B. and R.W.). C.G.-S. is supported by National Institutes of Health Grants RO1HL27255 and R21HL105383. L.L. is supported by Research Grant Project GR-2009-1524351 from the Young Research Program of Italy's Health Minister.

Disclosure Summary: The authors have nothing to disclose.

References

1. **Rossi GP, Sechi LA, Giacchetti G, Ronconi V, Strazzullo P, Funder JW.** Primary aldosteronism: Cardiovascular, renal and metabolic implications. *Trends Endocrinol Metab*. 2008;19(3):88–90.
2. **Rossi GP, Bernini G, Caliumi C, et al.** A prospective study of the prevalence of primary aldosteronism in 1,125 hypertensive patients. *J Am Coll Cardiol*. 2006;48(11):2293–2300.
3. **Rossi GP.** A comprehensive review of the clinical aspects of primary aldosteronism. *Nat Rev Endocrinol*. 2011;7:485–495.
4. **Choi M, Scholl UI, Yue Y, et al.** K+ channel mutations in adrenal aldosterone-producing adenomas and hereditary hypertension. *Science*. 2011;331(6018):768–772.
5. **Gomez-Sanchez CE, Oki K.** Minireview: potassium channels and aldosterone dysregulation. is primary aldosteronism a potassium channelopathy? *Endocrinology*. 2014;155(1):47–55.
6. **Hibino H, Inanobe A, Furutani K, Murakami S, Findlay I.** Inwardly rectifying potassium channels: their structure, function, and physiological roles. *Physiol Rev*. 2010;90:291–366.
7. **Boulkroun S, Beuschlein F, Rossi GP, et al.** Prevalence, clinical, and molecular correlates of KCNJ5 mutations in primary aldosteronism. *Hypertension*. 2012;59(3):592–598.
8. **Akerstrom T, Crona J, Delgado et al.** Comprehensive re-sequencing of adrenal aldosterone producing lesions reveal three somatic mutations near the KCNJ5 potassium channel selectivity filter. *PLoS One*. 2012;7(7):e41926.
9. **Taguchi R, Yamada M, Nakajima Y, et al.** Expression and mutations of KCNJ5 mRNA in Japanese patients with aldosterone-producing adenomas. *J Clin Endocrinol Metab*. 2012;97(4):1311–1319.
10. **Yamada M, Nakajima Y, Taguchi R, et al.** KCNJ5 mutations in aldosterone- and cortisol-co-secreting adrenal adenomas. *Endocr J*. 2012;59(8):735–741.
11. **Oki K, Plonczynski MW, Luis LM, Gomez-Sanchez EP, Gomez-Sanchez CE.** Potassium channel mutant KCNJ5 T158A expression in HAC-15 cells increases aldosterone synthesis. *Endocrinology*. 2012;153(4):1774–1782.
12. **Lenzini L, Caroccia B, Campos AG, et al.** Lower expression of the twik-related acid-sensitive K^+ channel 2 (TASK-2) gene is a hallmark of aldosterone producing adenoma causing human primary aldosteronism. *J Clin Endocrinol Metab*. 2014;99(4):E674–E682.
13. **Guagliardo NA, Yao J, Hu C, Barrett PQ.** Minireview: aldosterone biosynthesis: electrically gated for our protection. *Endocrinology*. 2012;153(8):3579–86.
14. **Belloni AS, Rossi GP, Andreis PG, et al.** Endothelin adrenocortical secretagogue effect is mediated by the B receptor in rats. *Hypertension*. 1996;27:1153–1159.
15. **Rossi GP, Albertin G, Belloni A, et al.** Gene expression, localization, and characterization of endothelin A and B receptors in the human adrenal cortex. *J Clin Invest*. 1994;94(3):1226–1234.
16. **Rossi GP, Cesari M, Letizia C, et al.** KCNJ5 gene somatic mutations affect cardiac remodelling but do not preclude cure of high blood pressure and regression of left ventricular hypertrophy in primary aldosteronism [published online April 22, 2014]. *J Hypertens*. doi: 10.1097/HJH.0000000000000186.
17. **Rossi GP, Seccia TM, Maniero C, Pessina AC.** Drug-related hypertension and resistance to antihypertensive treatment: a call for action. *J Hypertens*. 2011;29(12):2295–2309.
18. **Rossi GP, Belfiore A, Bernini G, et al.** Comparison of the captopril and the saline infusion test for excluding aldosterone-producing adenoma. *Hypertension*. 2007;50(2):424–431.
19. **Gomez-Sanchez CE, Qi X, Velarde-Miranda C, et al.** Development of monoclonal antibodies against human CYP11B1 and CYP11B2. *Mol Cell Endocrinol*. 2013;383(1–2):111–117.
20. **Sakuma I, Suematsu S, Matsuzawa Y, et al.** Characterization of steroidogenic enzyme expression in aldosterone-producing adenoma: a comparison with various human adrenal tumors. *Endocr J*. 2013;60(3):329–336.
21. **Fink M, Lesage F, Duprat F, et al.** A neuronal two P domain K+ channel stimulated by arachidonic acid and polyunsaturated fatty acids. *EMBO J*. 1998;17(12):3297–3308.
22. **Seccia TM, Mantero F, Letizia C, et al.** Somatic mutations in the KCNJ5 gene raise the lateralization index: implications for the diagnosis of primary aldosteronism by adrenal vein sampling. *J Clin Endocrinol Metab*. 2012;97(12):E2307–E2313.
23. **Arnold K, Bordoli L, Kopp J, Schwede T.** The SWISS-MODEL workspace: a web-based environment for protein structure homology modelling. *Bioinformatics*. 2006;22(2):195–201.
24. **Emsley P, Cowtan K.** 2004 Coot: model-building tools for molecular graphics. *Acta Crystallogr D Biol Crystallogr* 60(Pt 12 Pt 1):2126–2132.
25. **Brunger AT.** Version 1.2 of the crystallography and NMR system. *Nat Protoc*. 2007;2(11):2728–2733.
26. **Heginbotham L, Lu Z, Abramson T, MacKinnon R.** Mutations in the K+ channel signature sequence. *Biophys J*. 1994;66(4):1061–1067.
27. **Tauber P, Penton D, Tegtmeier I, et al.** Pharmacology and pathophysiology of mutated KCNJ5 found in adrenal aldosterone producing adenomas. *Endocrinology* 2014:155(4):1353–1362.
28. **Mulatero P, Tauber P, Zennaro M, et al.** KCNJ5 mutations in European families with nonglucocorticoid remediable familial hyperaldosteronism. *Hypertension*. 2012;59(2):235–240.
29. **Scholl UI, Nelson-Williams C, Yue P, et al.** Hypertension with or without adrenal hyperplasia due to different inherited mutations in the potassium channel KCNJ5. *Proc Natl Acad Sci USA*. 2012;109(7):2533–2538.
30. **Williams TA, Monticone S, Schack VR, et al.** Somatic ATP1A1, ATP2B3, and KCNJ5 mutations in aldosterone-producing adenomas. *Hypertension*. 2014;63(1):188–195.
31. **Monticone S, Hattangady NG, Penton D, et al.** A novel Y152C KCNJ5 mutation responsible for familial hyperaldosteronism type III. *J Clin Endocrinol Metab*. 2013;98(11):E1861–E1865.
32. **Monticone S, Hattangady NG, Nishimoto K, et al.** Effect of KCNJ5 mutations on gene expression in aldosterone-producing adenomas and adrenocortical cells. *J Clin Endocrinol Metab*. 2012;97(8):E1567–E1572.
33. **Azizan EAB, Murthy M, Stowasser M, et al.** Somatic mutations affecting the selectivity filter of KCNJ5 are frequent in 2 large unselected collections of adrenal aldosteronomas. *Hypertension*. 2012;59(3):587–591.
34. **Azizan EAB, Poulsen H, Tuluc P, et al.** Somatic mutations in ATP1A1 and CACNA1D underlie a common subtype of adrenal hypertension. *Nat Genet*. 2013;45(9):1055–1060.
35. **Murthy M, Azizan EAB, Brown MJ, O'Shaughnessy KM.** Characterization of a novel somatic KCNJ5 mutation delI157 in an aldosterone-producing adenoma. *J Hypertens*. 2012;30(9):1827–1833.
36. **Charmandari E, Sertedaki A, Kino T, et al.** A novel point mutation in the KCNJ5 gene causing primary hyperaldosteronism and early-onset autosomal dominant hypertension. *J Clin Endocrinol Metab*. 2012;97:1–8.
37. **Murthy M, Xu S, Massimo G, et al.** Role for germline mutations and a rare coding single nucleotide polymorphism within the KCNJ5 potassium channel in a large cohort of sporadic cases of primary aldosteronism. *Hypertension*. 2014;63(4):783–789.
38. **Anderson P, Bondesson U, Sylvén C, Aström H.** Plasma concentration-response relationship of verapamil in the treatment of angina pectoris. *J Cardiovasc Pharmacol*. 1982;4(4):609–614.
39. **Kuo A, Gulbis JM, Antcliff JF, et al.** Crystal structure of the potassium channel KirBac1.1 in the closed state. *Science*. 2003; 300(5627):1922–1926.
40. **Dibb KM, Rose T, Makary SY, et al.** Molecular basis of ion selectivity, block, and rectification of the inward rectifier Kir3.1/Kir3.4 K(+) channel. *J Biol Chem*. 2003;278(49):49537–49548.